Journal of Alloys and Compounds 495 (2010) 63–66

Contents lists available at ScienceDirect

Journal of Alloys and Compounds

journal homepage: www.elsevier.com/locate/jallcom

Review

Synthesis and characterization of shape-controlled $Ni_{0.5}Zn_{0.5}Fe_2O_4$ via the coprecipitation method

Qiaoling Li*, ChuanBo Chang, HongXia Jing, YongFei Wang

Department of Chemistry, School of Science, North University of China, Taiyuan 030051, China

ARTICLE INFO

Article history:
Received 22 September 2009
Received in revised form 7 January 2010
Accepted 9 January 2010
Available online 18 January 2010

Keywords:
Inorganic compounds
Electron microscopy
Magnetic properties
X-ray diffraction

ABSTRACT

Fe^{3+} was used for preparing spherical $Ni_{0.5}Zn_{0.5}Fe_2O_4$ with an average diameter of 40 nm by the coprecipitation method. Fe^{2+} and various precipitators (NaOH, Na_2CO_3 and $NH_3{\cdot}H_2O$) were used for preparing doped FeOOH with different morphologies and crystal types by the coprecipitation–air oxygenation method. Spindle-like and rod-like size-controlled $Ni_{0.5}Zn_{0.5}Fe_2O_4$ samples were obtained subsequent to the calcinations of the precursor, for $Ni_{0.5}Zn_{0.5}Fe_2O_4$ maintained the morphology of the doped FeOOH. The phase, morphology, and particle diameter of the samples were studied by X-ray diffraction (XRD) and transmission electron microscopy (TEM), and the magnetic properties were measured by a vibrating sample magnetometer (VSM). It was found that the coercivity of the sample increased with an increase in the effective anisotropy. Also, the comprehensive magnetic properties of the samples obtained via Fe^{2+} and the NaOH precipitator were optimum, and the coercivity, saturation magnetization, and remanent magnetization for the $Ni_{0.5}Zn_{0.5}Fe_2O_4$ sample were obtained as 90.5 Oe, 54.3 emu/g, and 5.1 emu/g, respectively.

Contents

1. Introduction

Recently, nanostructured materials have been the focus of scientific research due to their fundamental significance for physical properties and potential application in nanodevices [1–4]. Among nanomaterials with different structures, one-dimensional (1D) nanostructured materials have received tremendous attention because of their unique properties derived from their low dimensionality [5]. These 1D nanostructured materials have found application of fabricating nanoscale electronic, magnetic, and optical devices [6]. Especially, the synthesis of 1D nanostructured magnetic materials is a very important area of research, because of their applications in high-density magnetic storage media, biomolecular separations and magnetic carriers for drug targeting [7]. As one of the most important nanostructured magnetic materials, spinel nickel–zinc ferrite have been developed into a wide range of applications in high-density magnetic recording, ferrofluids technology, biomedical drug delivery, and magnetic resonance imaging (MRI) [8,9]. Spinel nickel–zinc ferrite can be synthesized by various methods such as the sol–gel method [10], ball milling method [11], hydrothermal method [12], combustion method [13], mechano-chemical method [14], precursor method [15], and microemulsion method [16]. However, the preparation of one-dimensional (1D) nanostructured $Ni_{0.5}Zn_{0.5}Fe_2O_4$ remains a challenge because the high symmetry of spinel structure unfavorably induces the 1D growth without extra restriction, particularly the synthesis by the coprecipitation method, has been seldom reported.

In this study, $Ni_{0.5}Zn_{0.5}Fe_2O_4$ nanomaterials of different shapes and sizes were successfully prepared via the coprecipitation method by the use of different precipitators and different ferric

* Corresponding author. Tel.: +86 351 3923197; fax: +86 351 3922152.
E-mail address: qiaolingl@163.com (Q. Li).

0925-8388/$ – see front matter © 2010 Elsevier B.V. All rights reserved.
doi:10.1016/j.jallcom.2010.01.034

salts. An easy synthesis procedure was carried out by using a simple apparatus, and the products were well-dispersed. The morphology, phase, and magnetic properties of the $Ni_{0.5}Zn_{0.5}Fe_2O_4$ nanomaterials were studied. In addition, the mechanism of the influence of the precipitator on the morphology and the variation in the magnetic properties of $Ni_{0.5}Zn_{0.5}Fe_2O_4$, were preliminarily studied.

2. Experimental details

$FeCl_3$, $Ni(NO_3)_2$, and $Zn(NO_3)_2$ were weighed according to the formula of $Ni_{0.5}Zn_{0.5}Fe_2O_4$. Subsequently, the above mixture together with a little polyglycol was dissolved in deionized water (40 ml) and stirred in a magnetic blender at 40 °C. NaOH was dissolved in another deionized water (40 ml). The NaOH solution was dipped into the intermixture of $Ni(NO_3)_2$ and $Zn(NO_3)_2$ (the dipping time was controlled in 1 h, and the pH value was kept over 12). The above intermixture was stirred in a magnetic blender at 40 °C for 5 h. The product was then filtered and washed several times until the washed liquid was neutral. The precipitate was dried in a cabinet dryer at 80 °C for 12 h to obtain the precursor samples. The precursor samples were calcined for 2 h at temperatures of 500 °C, 600 °C, and 700 °C, respectively. Thus, the spherical $Ni_{0.5}Zn_{0.5}Fe_2O_4$ samples were obtained.

An appropriate amount of $FeCl_2$ and a small amount of polyglycol were dissolved in deionized water, and stirred in the magnetic blender at 40 °C to obtain $FeCl_2$ solution. The pH value of the $FeCl_2$ solution was adjusted between 12 and 14 by using the precipitators (NaOH, Na_2CO_3, or $NH_3{\cdot}H_2O$) to obtain solution A. According to the formula of $Ni_{0.5}Zn_{0.5}Fe_2O_4$, $Zn(NO_3)_2$ and $Ni(NO_3)_2$ were dissolved in appropriate amount of deionized water to obtain solution B. Subsequently, solution B was dripped into solution A. The dripping rate was controlled at about one gutta per 2 s. After the dripping process, the mixture was stirred for 6 h. The product was then filtered and washed several times until the washing liquid was neutral. The precipitate was dried in the cabinet dryer at 80 °C for 12 h to obtain the precursor FeOOH samples. The precursor samples were calcined for 2 h at temperatures of 500 °C, 600 °C, and 700 °C, respectively. Thus, $Ni_{0.5}Zn_{0.5}Fe_2O_4$ samples of different shapes were obtained.

The synthesized samples were subsequently characterized by X-ray diffraction (XRD, Rigaku D/max-gB X-ray diffractometer with Cu Ka radiation), and transmission electron microscopy (TEM, H-800). The magnetic properties were measured by a vibrating sample magnetometer (VSM) at a room temperature under a maximum field of 15 T.

3. Results and discussion

The phase identification of the precursor and the as-prepared $Ni_{0.5}Zn_{0.5}Fe_2O_4$ samples was examined by XRD. The XRD pattern of precursor obtained by Fe^{3+} and NaOH precipitator is shown in Fig. 1A. It can be seen that these peaks were indexed to the $Fe(OH)_3$ phase according to the standard JCPDS (Card No. 24-1207), which indicates that the precursor samples obtained by this

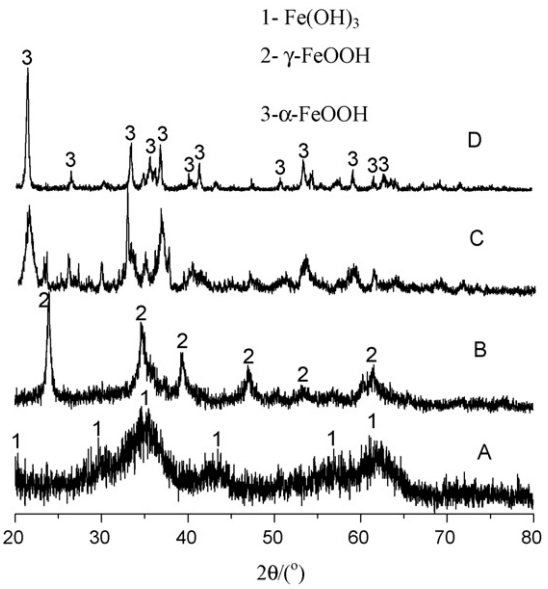

Fig. 1. The XRD pattern of different precursors.

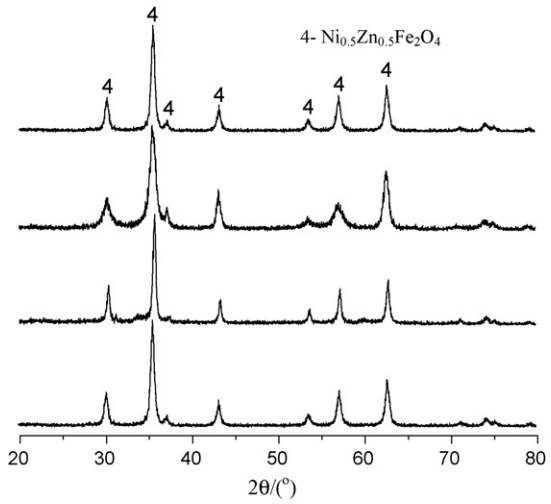

Fig. 2. The XRD pattern of the as-synthesized $Ni_{0.5}Zn_{0.5}Fe_2O_4$ obtained by the annealing of the precursors that of Fig. 1 at 600 °C.

method were $Fe(OH)_3$. The XRD patterns of precursors obtained by $FeCl_2$ and three precipitators (Na_2CO_3, $NH_3{\cdot}H_2O$, or NaOH, respectively) are shown in Fig. 1B–D. The contrast between the XRD characteristic peaks and the standard JCPDS indicates that the precursor obtained by Na_2CO_3 precipitator was pure γ-FeOOH, and that obtained by $NH_3{\cdot}H_2O$ precipitator was a mixture of α-FeOOH and γ-FeOOH. Also, the precursor obtained by NaOH precipitator was α-FeOOH. Further, no characteristic peaks of impurities were detected, which indicates that the Ni^{2+} and Zn^{2+} existed in the crystal lattice of the precursor. The XRD pattern of the as-synthesized $Ni_{0.5}Zn_{0.5}Fe_2O_4$ is shown in Fig. 2A–D, which was obtained by annealing the precursors according to Fig. 1 at 600 °C. The contrast between the XRD characteristic peaks of the obtained samples and the standard JCPDS of $Ni_{0.5}Zn_{0.5}Fe_2O_4$ indicates that no characteristic peaks of impurities were detected in the four spectrums, and pure $Ni_{0.5}Zn_{0.5}Fe_2O_4$ samples were obtained.

The morphology and particle sizes of the precursor and the as-prepared samples were characterized by TEM. The TEM images of the precursor and the $Ni_{0.5}Zn_{0.5}Fe_2O_4$ sample are shown in Figs. 3 and 4, respectively. The TEM images of the precursor and the $Ni_{0.5}Zn_{0.5}Fe_2O_4$ sample obtained by Fe^{3+} and NaOH precipitators are shown in Figs. 3A and 4A, respectively. It was found from the TEM images that the precursor and the $Ni_{0.5}Zn_{0.5}Fe_2O_4$ sample had well-dispersed spherical morphology with an average diameter of about 40 nm. The diameter of the sample increased slightly following the calcination process. The TEM images of the precursor obtained by $FeCl_2$ and three precipitators ($NH_3{\cdot}H_2O$, Na_2CO_3, and NaOH, respectively) are shown in Fig. 3B–D. The TEM images of $Ni_{0.5}Zn_{0.5}Fe_2O_4$ samples corresponding to the precursor in Fig. 3B–D are shown in Fig. 4B–D. Compared with the sample obtained by $FeCl_3$, the morphology of the sample obtained by $FeCl_2$ developed into one-dimensional structure obviously. The samples through $NH_3{\cdot}H_2O$ precipitator had spindle-like morphology with an average diameter and an aspect ratio of 30 nm and 3, respectively. When $NaCO_3$ was used as the precipitator, the morphology of the samples remained spindle-like. However, the average diameter and the aspect ratio of the samples increased to 50 nm and 5, respectively. As shown in Figs. 3D and 4D, the precursor obtained by NaOH precipitator had rod-like structure with an average diameter and an aspect ratio of about 30 nm and 20, respectively. By comparing the TEM images of the precursor and the $Ni_{0.5}Zn_{0.5}Fe_2O_4$ sample, it was found that their morphologies were similar. The grain size of the formed $Ni_{0.5}Zn_{0.5}Fe_2O_4$ was slightly higher than that of the precursor.

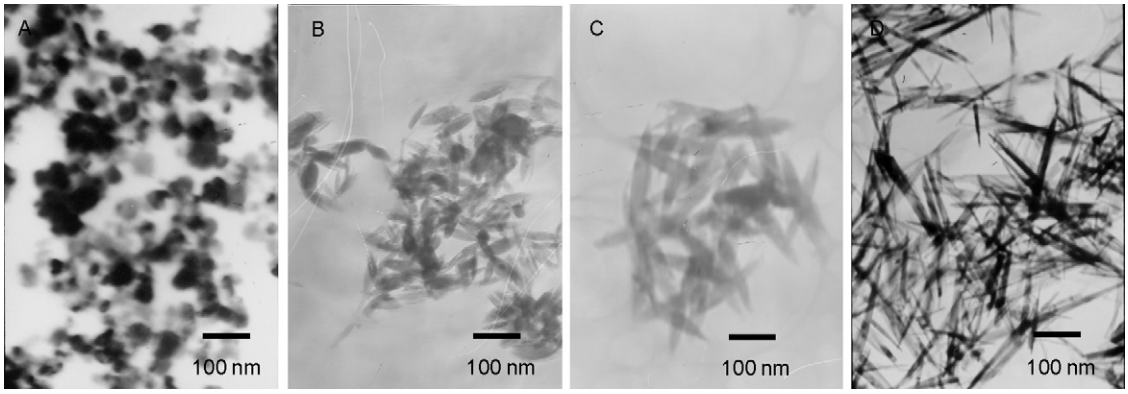

Fig. 3. The TEM images of different precursors.

Olowe et al. [17] considered that at the room temperature, the ultimate oxidation product of Fe(II) depended on the mol ratio of $Fe^{2+}$and the precipitator [$R = n(Fe^{2+})/n$(precipitator)] in the $Fe^{2+}$and alkalescence system. The product could be α-FeOOH for R lower than 0.500, α-FeOOH and Fe_3O_4 for R ranging between 0.500 and 0.583, and α-FeOOH and γ-FeOOH for R higher than 0.625. As shown in Ref. [18], three existent forms (Fe^{2+}, $Fe(OH)^+$, $Fe(OH)_2$) of Fe^{2+} were found in the preparation process of the FeOOH by the alkali method. Morgan and Lahav [19] reported that the reductive property of Fe^{2+} increased by combining with OH^-,owing to its higher electron density which could provide electron by σ and π bond. The reductive property ranking was observed as follows: $Fe(OH)_2 > Fe(OH)^+ > Fe^{2+}$, that is, the $Fe(OH)_2$ was most prone to be oxidized, whereas Fe^{2+} was most difficult to be oxidized. Thus, it was found that the pH value of the system affected the concentration of $Fe(OH)_2$ and further affected the oxidation rate of the system. As an orthogonal crystal type, the FeOOH was prone to develop into a one-dimensional structure [20]. Meanwhile, the aspect ratio of FeOOH has close relationship with the reaction rate in the system. At the primary stage, more nucleuses and thinner and longer powders were formed by accelerating and the aspect ratio of obtained samples is relatively larger. On the contrary, if the reaction rate was accelerated at the intermediate and later stage of the system, the obtained sample became shorter and thicker with the aspect ratio decreasing. Thus, one-dimensional spiculate α-FeOOH was obtained by NaOH precipitator for the higher reaction rate resulting from the lower R value. When Na_2CO_3 and $NH_3{\cdot}H_2O$ (R was higher than 0.625 and pH value ranging between 10 and 14) [21] were chosen as the precipitators, the pH value of the system was found to be lower for the lower release rate of OH^-, resulting in the lower transformation rate from Fe^{2+} to FeOOH. So, FeOOH core was formed gradually in the subsequent dissolution and recrystallization process, which prevented the one-dimensional growth of the FeOOH and further reduced the aspect ratio of the obtained FeOOH. Thus, spindle-like FeOOH with higher grain size was obtained. It was found that the aspect ratio of the precursor obtained by Na_2CO_3 precipitator was higher than that of the precursor obtained by $NH_3{\cdot}H_2O$ precipitator for $R = 0.625 < [n(Fe^{2+})/n(Na_2CO_3)] < [n(Fe^{2+})/n(NH_3{\cdot}H_2O)]$. The different morphologies of the precursors were maintained subsequent to the calcination process at 600 °C. Kakizaki [22] prepared $BaFe_{12}O_{19}$ by α-FeOOH, and found that the morphology of the obtained samples was the same as that of the α-FeOOH precursor. This conclusion is in accordance with the result obtained in this study.

Table 1
Magnetization measurement of the as-prepared $Ni_{0.5}Zn_{0.5}Fe_2O_4$ samples.

X	Coercivity (Hc)/Oe	Remanent magnetization (Mr)/(emu g^{-1})	Saturation magnetization (Ms)/(emu g^{-1})
A	18.3	1.39	49.9
B	32.5	2.3	53.3
C	75.5	6.2	64.9
D	90.5	5.1	54.3

A–D represent the $Ni_{0.5}Zn_{0.5}Fe_2O_4$ samples corresponding to that of Fig. 4.

Magnetization measurement of the as-prepared sample was carried out by a vibrating sample magnetometer with a magnetic field up to 10 kOe. The magnetic properties of $Ni_{0.5}Zn_{0.5}Fe_2O_4$ are shown in Table 1. As indicated in Table 1, the coercivity of the spicule $Ni_{0.5}Zn_{0.5}Fe_2O_4$ prepared by NaOH precipitator was maximal (90.5 Oe), while the coercivity of the spindle-like $Ni_{0.5}Zn_{0.5}Fe_2O_4$ prepared by Na_2CO_3 precipitator was secondary

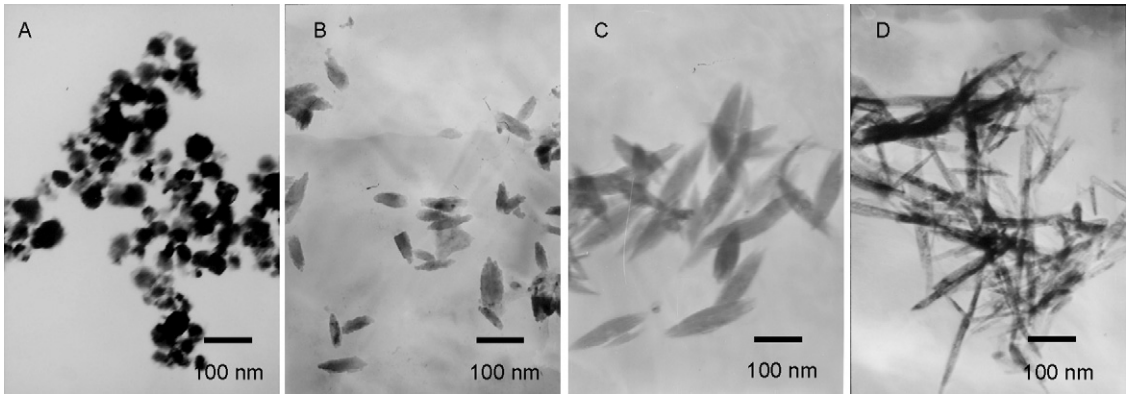

Fig. 4. The TEM images of different $Ni_{0.5}Zn_{0.5}Fe_2O_4$ samples.

(75.5 Oe). The coercivity of the spindle-like $Ni_{0.5}Zn_{0.5}Fe_2O_4$ prepared by $NH_3{\cdot}H_2O$ precipitator was 32.5 Oe which is lower than that prepared by Na_2CO_3 precipitator, and the coercivity of the sample obtained by $FeCl_3$ and NaOH was minimal (18.3 Oe). The differences in coercivity are mainly attributed to the differences in particle morphology [23]. As the higher shape anisotropy can significantly enhance the magnetic properties [7], a higher aspect ratio can favor the increase of the coercivity. The saturation magnetization and remanent magnetization of the sample were found to increase with increasing anisotropism of the sample. However, the variation was not very evident. The saturation magnetization of the $Ni_{0.5}Zn_{0.5}Fe_2O_4$ sample obtained by Na_2CO_3 precipitator was found to be higher than that of the other samples owing to its higher grain size. It has been reported that the particle size influences the magnetic properties of materials. It was found that Ms decreased with the decrease of crystallite size of mono-domain particles owing to the surface spin canting and thermal fluctuation [24,25].

4. Conclusions

The spherical $Ni_{0.5}Zn_{0.5}Fe_2O_4$ sample with an average diameter of 40 nm was obtained by the thermal treatment of the spherical doped $Fe(OH)_3$ precursor via the coprecipitation method. The spindle-like $Ni_{0.5}Zn_{0.5}Fe_2O_4$ sample with the grain size and aspect ratio of 30 nm and 3, the spindle-like $Ni_{0.5}Zn_{0.5}Fe_2O_4$ sample with the grain size and aspect ratio of 50 nm and 5, and the spicule $Ni_{0.5}Zn_{0.5}Fe_2O_4$ sample with the grain size and aspect ratio of 30 nm and 20 were prepared via the coprecipitation–air oxide method by Fe^{2+} and three different precipitators ($NH_3{\cdot}H_2O$, Na_2CO_3, and NaOH, respectively). The relationship between the morphology and the magnetic performance was observed, which indicated that the higher shape anisotropy could significantly enhance the magnetic properties. Thus, the coercivity of spicule nano-$Ni_{0.5}Zn_{0.5}Fe_2O_4$ was found to be the largest, about 90.5 Oe; the coercivities of spherical crystals were 75.5 and 32.5 Oe, respectively; and the coercivity of spherical nano-$Ni_{0.5}Zn_{0.5}Fe_2O_4$ was minimal (18.3), which was close to paramagnetism. In addition, it was observed that the saturation magnetization (Ms) values of $Ni_{0.5}Zn_{0.5}Fe_2O_4$ increased with an increase in the particle size of the sample.

Acknowledgments

The authors acknowledge the North University of China for the support given for carrying out this work under projects from the National Natural Science Fund (20571066; 20871108) and the projects of qualified personnel plan of the National and Province.

References

[1] Y. Yin, R.M. Rioux, C.K. Erdonmez, S. Hughes, G.A. Somorjai, A.P. Alivisatos, Science 304 (2004) 711–715.
[2] A.I. Hochbaum, R. Fan, R. He, P. Yang, Nano Lett. 5 (2005) 457–463.
[3] Z. Zhong, D. Wang, Y. Cui, M.W. Bockrath, C.M. Lieber, Science 302 (2003) 1377–1401.
[4] H.E. Zhang, B.F. Zhang, G.F. Wang, X.H. Dong, J. Magn. Magn. Mater. 312 (2007) 126–130J.
[5] Y.J. Wang, Y.J. Wu, P.Q. Zhu, Wang, Mater. Lett. 61 (2007) 1522–1525.
[6] D.G. Zhang, Z.W. Tong, G.Y. Xu, S.Z. Li, J.J. Ma, Solid State Sci. 11 (2009) 113–117.
[7] D.G. Zhang, X.F. Pan, N. Chen, K.K. Gan, M.Y. Gu, Mater. Res. Bull. 43 (2008) 1369–1375.
[8] E. Veena Gopalan, I.A. Al-Omari, K.A. Malini, P.A. Joy, D. Sakthi Kumar, J. Magn. Magn. Mater. 321 (2009) 1092–1099.
[9] X. Li, Q. Li, Z.G. Xia, W.X. Yan, J. Alloys Compd. 458 (2008) 558–563.
[10] H.E. Zhang, B.F. Zhang, G.F. Wang, X.H. Dong, Y. Gao, J. Magn. Magn. Mater. 312 (2007) 126–130.
[11] M. Jalaly, M.H. Enayati, F. Karimzadeh, J. Alloys Compd. 480 (2009) 737–740.
[12] S.M. Li, Q. Wang, A.B. Wu, Curr. Appl. Phys. 9 (2009) 1386–1392.
[13] A.C.F.M. Costa, A.M.D. Leite, H.S. Ferreira, J. Eur. Ceram. Soc. 28 (2008) 2033–2037.
[14] S. Dasgupta, K.B. Kim, J. Ellrichc, J. Alloys Compd. 424 (2006) 13–20.
[15] M. Gharagozlou, J. Alloys Compd. 486 (2009) 660–665.
[16] J.L. Zhang, J.X. Shi, M.L. Gong, J. Solid State Chem. 182 (2009) 2135–2140.
[17] A.A. Olowe, B. Pauron, J. Gbninrm, Corros. Sci. 52 (1991) 958–1001.
[18] J. Deng, R.F. Chen, G.Q. Song, Chin. J. Synth. Cryst. 37 (2008) 935–939.
[19] B. Morgan, O. Lahav, Chemosphere 66 (2007) 2080–2086.
[20] K.K. Sang, S.K. Shigeru, S. Masatoshi, Corros. Sci. 47 (2005) 2543–2549.
[21] Z. Meng, Z.B. Jia, J. Hebei. Normal Univ. 28 (2004) 432.
[22] K. Kakizaki, N. Hiratsuka, T. Namikawa, J. Magn. Magn. Mater. 176 (1997) 36–40.
[23] D. Li, T. Herricks, Y. Xia, Appl. Phys. Lett. 83 (2003) 4586–4590.
[24] M.B. Shelar, P.A. Jadhav, S.S. Chougule, M.M. Mallapur, B.K. Chougule, J. Alloys Compd. 476 (2009) 760–764.
[25] L. Rezlescu, E. Rezlescu, P.D. Popa, N. Rezlescu, J. Magn. Magn. Mater. 193 (1999) 288–294.